

Nonexponential Photon-Echo Decays of Paramagnetic Ions in the Superhyperfine Limit

Joseph Ganem, Y. P. Wang, D. Boye,^(a) R. S. Meltzer, and W. M. Yen
Department of Physics and Astronomy, University of Georgia, Athens, Georgia 30602

R. M. Macfarlane

IBM Research Almaden Laboratory, San Jose, California 95120

(Received 26 November 1990)

Nonexponential photon-echo decays are observed in ruby, $\text{Er}^{3+}:\text{YLiF}_4$, and $\text{Er}^{3+}:\text{LaF}_3$ with samples of low ion concentrations in high (10–50 kG) magnetic fields. At the highest fields, photon-echo decays are field independent and their temporal forms are identical for all three systems. This behavior is attributed to optical dephasing arising from electron-spin nuclear-spin superhyperfine interactions in the presence of a frozen core.

PACS numbers: 42.50.Md, 78.50.Ec

The optical dephasing of the electronic spins of paramagnetic ions reflects the temporal evolution of their spectrum arising from the dynamics of the environment. Dynamic processes result from interaction of the ions with other electron spins or with nuclear spins of the host. In most situations because of limited dynamical range of the experiments, echo decays are treated as exponential. However, it is well known that electron-spin-echo decay can show strong nonexponential character.¹ Such behavior is expected when the ions interact with other electron or nuclear spins and it is surprising that it has only recently been reported in the optical domain.^{2,3} It is the purpose of this paper to examine the optical dephasing of paramagnetic ions with large magnetic moments in the presence of only superhyperfine interactions with the neighboring nuclear spins. We show that, in this limit, highly nonexponential photon-echo decay is the general experimental result, the shape and rate of the decay becomes independent of magnetic field, and the temporal form of the decay is identical in the three systems studied. We discuss this result in terms of the dynamics of the frozen core of nuclear spins produced by the large magnetic moments of the paramagnetic spins. It is hoped that this work will provoke theoretical interest in examining whether there exists a universal decay envelope shape characterizing superhyperfine limited optical dephasing.

Recently, there have been reports of nonexponential photon-echo decays for ruby² and for $\text{Er}^{3+}:\text{YLiF}_4$ (Ref. 3) in high magnetic fields. In both systems there is a lengthening of the photon-echo decay and a gradual transition from exponential to nonexponential behavior associated with an increase in the magnetic field (B), a reduction in the temperature (T), and a decrease in the concentration of the optically active ions. All these share the property that they reduce the probability that an electron-spin flip nearby the coherently prepared ion will occur, by either reducing the spin-flip rate or the site occupancy. Superhyperfine-limited decay is characterized

by field-independent decay rates and is reached by reducing the dopant levels and increasing the field so that the dephasing from electron-spin–electron-spin interactions becomes negligible.⁴ In contrast, when electron-spin–electron-spin interactions control the dephasing, the decay times are strongly field dependent.^{2,3}

Two-pulse photon-echo experiments were conducted by gating a tunable single-frequency (1 MHz) cw dye laser. Pulses were produced with two acousto-optic modulators in tandem, the first gating the laser light into two pulses, while the second was gated off after the two-pulse sequence in order to provide additional rejection of laser light during the echo. The echo was detected with a photomultiplier tube that was protected during the preparation pulses with either a Pockels cell or another acousto-optic modulator. In all cases the pulses were collinear and propagated perpendicular to the c axis. Echoes were generated in three materials: 0.0014 at. % ruby with $\mathbf{B} \parallel \mathbf{c}$, 0.013 at. % $\text{Er}^{3+}:\text{YLiF}_4$ with $\mathbf{B} \perp \mathbf{c}$, and several $\text{Er}^{3+}:\text{LaF}_3$ samples (concentrations of 0.01, 0.03, and 0.1 at. %) with $\mathbf{B} \parallel \mathbf{c}$. Photon-echo decays were measured for the ${}^4A_2(-\frac{3}{2}) \leftrightarrow {}^2E(-\frac{1}{2})$ transition in ruby ($-\frac{3}{2}$ echo) using σ polarized pulses about 2 μsec wide. In $\text{Er}^{3+}:\text{YLiF}_4$ echoes were generated on the transition between the ground Zeeman sublevel of ${}^4I_{15/2}$ state and lowest Zeeman sublevel of the ${}^4F_{9/2}$ state using π polarized light and pulse lengths in the range of 0.2–0.9 μsec . For $\text{Er}^{3+}:\text{LaF}_3$ echo experiments were performed on the transition between the lowest Zeeman sublevels of the ${}^4I_{15/2}$ and ${}^4S_{3/2}$ states with 0.5- μsec pulses also π polarized.⁵ Echo decays were independent of laser intensity for pulse energies in the range of 4–12 nJ.⁶

The transition from exponential photon-echo decay, which is field and temperature dependent, to nonexponential behavior, which is field and temperature independent, is clearly seen in Fig. 1 for the $-\frac{3}{2}$ echo in ruby. In Fig. 1 echo intensities for 0.0014% ruby are compared to those reported previously² for 0.018% ruby at the same set of fields and temperatures. In contrast to

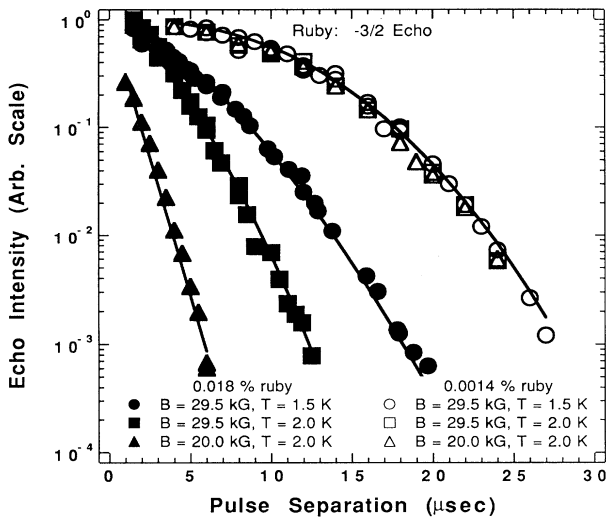


FIG. 1. Photon-echo decays for the $-\frac{3}{2}$ echo in ruby. Echo intensity (I) is shown vs pulse separation (τ). The open markers are echo intensities for the 0.0014% sample measured at a field of 29.5 kG and temperatures of 1.5 K (open circles), 2.0 K (open squares), and at 20 kG and 2.0 K (open triangles). Also shown are echo intensities at the exact same set of fields and temperatures for a 0.018% ruby sample taken from Ref. 2 (corresponding solid symbols).

the 0.018% sample, the photon-echo decays in 0.0014% ruby are longer and exhibit no variation in decay rate over the same range of fields and temperatures. The decay of the photon echo for the 0.0014% sample is nonexponential, while for the 0.018% sample decays are exponential at 20 kG and 2.0 K but begin a transition to nonexponential behavior as the field is raised and the temperature reduced.

Mims¹ provided a general description for the decay of electron spin echoes which takes the following form:

$$I = I_0 e^{-(4\tau/T_M)^x}. \quad (1)$$

The shape of the echo decay envelope is characterized by two parameters, the phase memory time T_M and an exponent x , which describes the echo decay shape. When $x=1$ the decay is exponential and $T_M=T_2$, the transverse dephasing time. Klauder and Anderson⁷ and Hu and Hartmann⁸ have shown that in the short-time limit applicable here ($\tau \ll$ spin-flip time), that $x=2$ for the "sudden-jump" model describing dephasing arising from single-ion electron-spin flips. Fits by Eq. (1) were made for the photon-echo decay data from the 0.0014% ruby, 0.013% $\text{Er}^{3+}:\text{YLiF}_4$, and all the $\text{Er}^{3+}:\text{LaF}_3$ samples. Also fitted by Eq. (1) were previously published echo decays in ruby² and $\text{Er}^{3+}:\text{YLiF}_4$.³

In each sample the echo decay becomes independent of field for B/T in excess of some critical value that depends on concentration. In all cases studied here, when this occurs, $x=2.4$ and a maximum value of the phase

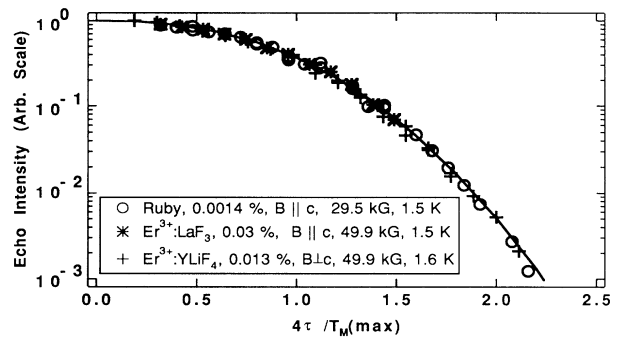


FIG. 2. Echo intensities in the superhyperfine limit for ruby, $\text{Er}^{3+}:\text{YLiF}_4$ (${}^4F_{9/2}$), and $\text{Er}^{3+}:\text{LaF}_3$ (${}^4S_{3/2}$) are shown vs $4\tau/T_M(\text{max})$, where $T_M(\text{max})$ is the maximum phase memory time for the system. The shapes of the echo decay envelopes are found to be identical. The solid curve shown is Eq. (1) with $x=2.4$.

memory time, $T_M(\text{max})$, is achieved. These values of $T_M(\text{max})$ are 50, 10, and 19 μsec for ruby ($\mathbf{B} \parallel \mathbf{c}$), $\text{Er}^{3+}:\text{YLiF}_4$ ($\mathbf{B} \perp \mathbf{c}$), and $\text{Er}^{3+}:\text{LaF}_3$ ($\mathbf{B} \parallel \mathbf{c}$), respectively. The universal character of the echo decay in these three systems is shown in Fig. 2 where an echo decay representative for each material at the highest values of B/T is plotted as a function of a dimensionless time argument expressed as $4\tau/T_M(\text{max})$. Note that each of these decays fits the same form of nonexponential decay described by Eq. (1) with $x=2.4$ (solid curve).

At temperatures between 1.5 and 2.0 K, phonon-induced transitions among the ground or excited states of the coherently prepared ions do not contribute to the dephasing.² Electron-spin-induced dephasing results from magnetic-field fluctuations produced by spin flips of the nearby paramagnetic ions. Under these conditions the critical value of B/T for which $T_M(\text{max})$ is achieved can be understood by calculating $(r_2)_{\text{av}}$, the average distance between the optically prepared ion and an ion in the first-excited Zeeman ground-state sublevel. There will be some critical value for $(r_2)_{\text{av}}$ for which the electron-spin-flip processes cannot compete with dephasing arising from the nuclear-spin dynamics; this is the superhyperfine limit.

The average nearest-neighbor distance is $r_{\text{av}} = (0.170/n)^{1/3}$, where n is the density of the ions.⁹ Therefore we can write the average distance between the coherently prepared ion and another impurity ion in the i th sublevel as

$$r_i(C, \mathbf{B}, T, g)_{\text{av}} = (0.170/n_0 C P_i)^{1/3}, \quad (2)$$

where n_0 is the number of atoms per unit volume in the pure crystal for which the impurity ions will substitute ($n_0 = 4.7 \times 10^{22} \text{ Al/cm}^3$ in ruby, $1.3 \times 10^{22} \text{ Y/cm}^3$ in YLiF_4 , and $1.8 \times 10^{22} \text{ La/cm}^3$ in LaF_3), C is the concentration of the impurity ions, and P_i is the fractional population of the i th sublevel. For a spin doublet such as

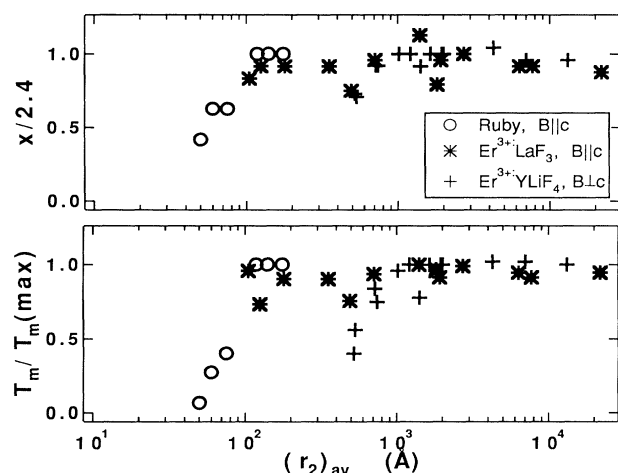


FIG. 3. The variation of T_M and x for ruby, $\text{Er}^{3+}:\text{YLiF}_4$ (${}^4F_{9/2}$), and $\text{Er}^{3+}:\text{LaF}_3$ (${}^4S_{3/2}$) as a function of $(r_2)_{\text{av}}$, the average distance between an optical center and an ion in the first-excited Zeeman ground sublevel.

Er^{3+} ,

$$P_i = e^{-g\mu_B B/kT}, \quad (3)$$

where k is the Boltzmann constant, μ_B is the Bohr magneton, and $g_{\perp} = 8.1$ for $\text{Er}^{3+}:\text{YLiF}_4$ and $g_{\parallel} = 8.05$ for $\text{Er}^{3+}:\text{LaF}_3$. For Cr^{3+} in ruby, the dependence on B and T is more complicated because of the quartet nature of the ground state and its zero-field splitting.

Figure 3 shows the experimental values of $x/2.4$ and $T_M/T_M(\text{max})$ as a function of $(r_2)_{\text{av}}$. We find for ruby and $\text{Er}^{3+}:\text{YLiF}_4$ a critical value of $(r_2)_{\text{av}}$, above which electron-spin-electron-spin interactions cease to contribute to the optical dephasing. For ruby at distances greater than 100 Å, x becomes constant at about 2.4 and T_M becomes equal to $T_M(\text{max})$. The critical value of $(r_2)_{\text{av}}$ for which this occurs in $\text{Er}^{3+}:\text{YLiF}_4$ is about 700 Å. We have not determined the critical distance for $\text{Er}^{3+}:\text{LaF}_3$ but it seems to be no greater than 200 Å. A critical distance of a few hundred Å for the transition to the superhyperfine limit is consistent with Bloembergen's estimate that the electron-spin-electron-spin interactions between paramagnetic ions is negligible when the average distance between the ions becomes much greater than 10^2 Å.¹⁰

We believe that the nonexponential nature of photon-echo decays in the superhyperfine limit arises because of the "frozen-core" effect.¹¹⁻¹³ The large magnetic moments of the optically active ions detune the neighboring nuclear spins from one another with the resonant energy mismatch increasing with a decrease in distance to the optical ion. This results in a distribution of mutual nuclear-spin-flip rates with the rate decreasing from the bulk value far from the electron spin to a very slow rate for spins near the ion.¹⁴ At early times only nuclear

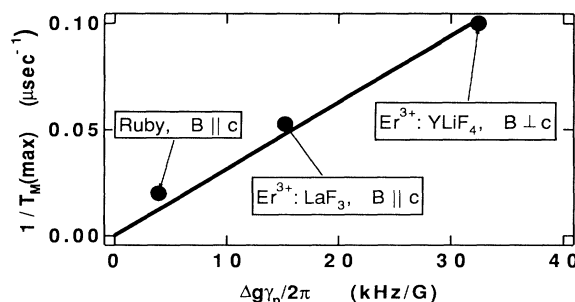


FIG. 4. Reciprocal phase memory times in the superhyperfine limit $1/T_M(\text{max})$ for ruby, $\text{Er}^{3+}:\text{YLiF}_4$ (${}^4F_{9/2}$), and $\text{Er}^{3+}:\text{LaF}_3$ (${}^4S_{3/2}$) are shown vs $\Delta g\gamma_n$. The best-fit line through the origin has a slope of 0.5 G/rad.

spins far from the optical ion have flipped but eventually nearby spins, which interact more strongly with the electronic spin, will also flip. This produces a nonexponential optical dephasing.

The variation of $T_M(\text{max})$ can be understood in terms of the strength of the magnetic dipole-dipole interaction between the nuclear and electronic spins. The magnetic dipole moment of the nucleus is given by $\mu_n = \gamma_n \hbar I$, where γ_n is the gyromagnetic ratio of the nucleus which has values for $\gamma_n/2\pi$ of 4.01 kHz/G for F and 1.11 kHz/G for Al. The effective magnetic-moment difference of the echo producing electronic-spin state is $\mu_e = \frac{1}{2}(\Delta g)\mu_B S$, where Δg , the difference between the electronically excited and ground state g values, is 3.52 (pseudospin = $\frac{1}{2}$) for ruby ($\mathbf{B} \parallel \mathbf{c}$), 3.8 for $\text{Er}^{3+}:\text{LaF}_3$ ($\mathbf{B} \parallel \mathbf{c}$), and 8.1 ± 0.2 for $\text{Er}^{3+}:\text{YLiF}_4$ ($\mathbf{B} \perp \mathbf{c}$). Since one needs to consider only the energy needed to produce changes in m_l and m_s of ± 1 , we expect the dephasing rate to scale with the product $\Delta g\gamma_n$. Figure 4 shows that $1/T_M(\text{max})$ for each of the three systems is approximately linear in $\Delta g\gamma_n$ with a best-fit line through the origin having a slope of 0.5 G/rad.

For ions with large magnetic moments such as the Kramers systems described here, the superhyperfine limit is characterized by an optical dephasing in which the photon-echo decay envelope at low temperatures and high magnetic fields becomes highly nonexponential and independent of B and T . The form of the nonexponential decay is identical in three systems, two of which are Er^{3+} -doped fluorides and the other is a Cr^{3+} -doped oxide, suggesting that the observed behavior should be widespread or even general in such systems. The observed scaling of $1/T_M(\text{max})$ with $\Delta g\gamma_n$ in the three systems, in spite of their different structural details, provides further evidence for the generality of these results and points to the role of the frozen core. In the present case of large electron magnetic moments, nuclear spins in close proximity to the paramagnetic ion remain dynamically frozen during the echo decay.¹⁴ Optical dephasing results from interaction with nuclear spins relatively far from the ion where the structural details be-

come unimportant. Structural details should be important in systems containing ions with small magnetic moments where the frozen core would be much smaller.

The exact form of the echo decay is determined by the temporal broadening of the spectral distribution of the coherently prepared ensemble. In the sudden-jump model for electron spins, the spin-flip rates are independent of their location relative to the coherently prepared ions leading to nonexponential decay with $x=2$. For nuclear spin flips in the frozen core the correlation of the flip rates with position results in a more highly nonexponential echo decay with $x=2.4$. We conclude that the melting of the core must broaden the spectral distribution of these systems in a similar fashion producing the observed general behavior. The value of the parameter, x , which characterizes the nonexponential photon-echo decay contains the detailed information on the dynamics of the frozen core.

We thank Kiwan Jeng for assistance. We also thank J. I. Dijkhuis for providing the 0.0014% ruby crystal. This research has been funded in part by the NSF under Grant No. DMR-8717696 and by the University of Georgia Research Foundation.

^(a)Present address: Physics Department, Davidson College, Davidson, NC 28036.

¹W. B. Mims, *Phys. Rev.* **168**, 370 (1968).

²Joseph Ganem, Y. P. Wang, R. S. Meltzer, and W. M. Yen, *Phys. Rev. B* (to be published).

³R. M. Macfarlane, R. Wannemacher, D. Boye, Y. P. Wang, and R. S. Meltzer (to be published).

⁴Although in small fields superhyperfine contributions to the dephasing are field dependent, the field dependence saturates in large fields when the nuclear spins interact more strongly with the field than with each other. See L. Q. Lambert, *Phys. Rev. B* **7**, 1834 (1973).

⁵R. M. Macfarlane and R. M. Shelby, *Opt. Commun.* **42**, 346 (1982). For $\text{Er}^{3+}:\text{LaF}_3$ the echo decays themselves were never published, but rather the results of fits to an exponential function. The decays in $\text{Er}^{3+}:\text{LaF}_3$ are in fact nonexponential and fits to these data were made using Eq. (1).

⁶In order to have the dynamic range necessary to measure the entire echo decay it was not possible to reduce pulse energies further. Intensity-dependent dephasing has been reported for gated cw echoes [see Jin Huang, J. M. Zhang, and T. W. Mossberg, *Opt. Commun.* **75**, 29 (1990)]. These effects are found to diminish as the number of excited ions is reduced. Our samples are much more dilute than those for which these effects were reported. We are exciting a factor of 10 less ions in $\text{Er}^{3+}:\text{LaF}_3$ and $\text{Er}^{3+}:\text{YLiF}_4$ and a factor of 10^3 less in ruby. Therefore at the low concentrations and the low power levels that we used, any intensity-dependent dephasing should be negligible.

⁷J. R. Klauder and P. W. Anderson, *Phys. Rev.* **125**, 912 (1962).

⁸P. Hu and S. R. Hartmann, *Phys. Rev. B* **9**, 1 (1974).

⁹S. K. Lyo, *Phys. Rev. B* **3**, 3331 (1971).

¹⁰N. Bloembergen, *Physica (Utrecht)* **25**, 386 (1949).

¹¹R. M. Shelby, C. S. Yannoni, and R. M. Macfarlane, *Phys. Rev. Lett.* **41**, 1739 (1978).

¹²R. G. DeVoe, A. Wokaun, S. C. Rand, and R. G. Brewer, *Phys. Rev. B* **23**, 3125 (1981).

¹³A. Szabo, *Opt. Lett.* **8**, 486 (1983).

¹⁴A. Szabo, T. Muramoto, and R. Kaarli, *Phys. Rev. B* **42**, 7769 (1990).